Phase diagram of the three-dimensional Heisenberg antiferromagnet in the presence of a longitudinal field

Minos A. Neto[1], J. Roberto Viana[1], and J. Ricardo de Sousa[1,2]

[1]*Departamento de Física, Universidade Federal do Amazonas, 3000, Japiim, 69077-000, Manaus-AM, Brazil*

[2]*National Institute of Science and Technology for Complex Systems, Universidade Federal do Amazonas, 3000, Japiim, 69077-000, Manaus-AM, Brazil*

(Dated: May 3, 2009)

Abstract

The improved treatment developed by Bublitz and de Sousa [*Phys. Lett. A* **323,** 9 (2004)], the differential operator technique in the effective field theory (EFT) with finite cluster of $N = 2$ spins (EFT-2) and used to describe the phase diagram in the $T - H$ plane on the quantum spin-1/2 Heisenberg antiferromagnet in the presence of a longitudinal field (H) on a simple cubic (sc) lattice, is herein extended for larger clusters ($N = 4$ spins, EFT-4) to study the criticality on the sc and body centered cubic (bcc) lattices. For the sc ($z = 6$) lattice we obtain by using EFT-4 at null temperature ($T = 0$) the critical field ($H_c = 5.85J$) smaller that the classical value $H_c = 6J$, while EFT-2 found $H_c = 6.24J$. In the case of the bcc ($z = 8$) lattice we have observed for this quantum model a reentrant behavior around the critical field, which was also observed in the Ising antiferromagnet [Neto and de Sousa, *Phys. Rev. B* **70**, 224436 (2004)].

PACS numbers: 72.72.Dn; 75.30.Kz; 75.50.El

I. INTRODUCTION

The quantum spin-1/2 Heisenberg antiferromagnetic model (HAM) has been exhaustively studied by using several approximative methods[1–10]. The aim motivation to study this quantum model is its importance in the description of magnetic properties of antiferromagnetic compounds with localized magnetic moments (insulating), in particular, the undoped La_2CuO_4 compound[1]. When doped with holes, this compound (i.e., $La_{2-x}Sr_xCuO_4$) becomes high-temperature superconducting ($x > 2,5\%$)[11], whose physics is thought to be dominate by CuO planes, with only one CuO plane per unit cell and does not have the complications of chains. Anderson[12] original suggestion that novel quantum spin fluctuations in the CuO planes, common in al these doped cuprates, is responsible for the superconductivity. Therefore, the study of the properties of the CuO planes in La_2CuO_4 helps in the understanding of the whole class of superconducting cuprates.

The competition between the antiferromagnetic exchange interaction and the alignment of the local moments with the external field presents interesting properties in the phase diagram in the $T - H$ plane, for example, *reentrance phenomenon*, *multicritical points*, *successive phase transitions*, etc. In the case of the classical Ising antiferromagnetic model (IAM), only second order phase transitions are observed for all values of field H in the interval between $H = 0$ and $H = H_c = zJ$ at $T = 0$ (ground state), where J is the exchange interaction and z the coordination number. Around the critical field $H = H_c$, the phase diagram shows some qualitative differences, dependent on the dimensionality (d) and symmetry of the lattice. In non-frustrated two-dimensional lattices, the critical temperature $T_N(H)$ decreases with an increase of H, going to zero at $H = H_c$. The theoretical phase diagram on a square lattice is in accordance with the experimental results of the quasi-two-dimensional $CoCs_3Br_5$ compound[13].

From a theoretical point of view, an interesting property in the IAM in the presence of a longitudinal field is the sign of the slope of the phase boundary at $T = 0$, i.e., $a_c = \left(\frac{dH}{dT}\right)_{H=H_c}$. In 2d lattices the slope is always negative ($a_c < 0$), while for 3d lattice $a_c \geq 0$, depending on the value of z (topology of the lattice). We can estimate the values for the slope of the phase boundary[14]; for example, we have a_c(square lattice-**sq**)$= -0.67$, a_c(simple cubic lattice-**sc**)$= 0$ and a_c(body-centered cubic lattice-**bcc**)$= 0.13$, indicating that the critical curve $T_N(H)$ for the bcc lattice shows a reentrant behavior in the low-temperature (high-

field) region. Results using series expansion (SE)[14], Monte Carlo simulation (MC)[15] and renormalization group (RG)[16] have observed this reentrant behavior in the phase diagram on a bcc lattice, while for the sc lattice all this methods found $a_c = 0$ (no reentrance).

On the other hand, the phase diagram of the 3d HAM in an external field is not completely known. Calculations of high-temperature series expansion[17] and variational treatment[18] have obtained the critical behavior $T_N(H)$ in the high-field and low-field regions, respectively. Recently, Bublity and de Sousa[19] studied the phase diagram in the $T - H$ plane in all interval of field $H \in [0, H_c]$ on a sc lattice by using an effective-field theory in cluster with $N = 2$ spins (EFT-2). Due to quantum fluctuations, the critical field found is different from the classical value $H_c = 6J$. Usually quantum fluctuations reduces the critical values in comparison with classical ones; therefore, this larger value found for $H_c = 6.24J$ can be due to a finite-size effect, since a small cluster ($N = 2$ spins) was used. The field-induced quantum phase transition has been analyzed intensively in one-dimensional quantum spin models. For example, the ground state for the 1d HAF in a longitudinal field was studied by using density matrix renormalization group (DMRG)[20], where a fixed field $H_c = 1.883J$ smaller than the classical value $H_c = 2J$ is found. To our knowledge, few people have studied the 3d HAM in the presence of a longitudinal field[17–19].

In this work, first we develop the EFT in a larger cluster ($N = 4$ spins) to study the phase diagram of the HAM on a sc lattice, where our aim objective is to obtain the value of the critical field and verify if $H_c < 6J$. Another interesting critical behavior in this quantum model is to analyze the existence or not of reentrance in the phase diagram on a bcc lattice, where this reentrant phenomenon was observed in the IAM case[14–16]. In Section II, the model and the formalism are detailed. The phase diagram in the $T - H$ plane is discussed in Section III on three-dimensional (sc and bcc) lattices. Finally, in Section IV we present the conclusions.

II. MODEL AND FORMALISM

In this work we consider the nearest-neighbor (nn) Heisenberg antiferromagnet in the presence of a longitudinal field divided into two equivalent interpenetrating sublattices, A

and B, which is described by the following Hamiltonian:

$$\mathcal{H} = J \sum_{<i,j>} \boldsymbol{\sigma}_i \cdot \boldsymbol{\sigma}_j - H \sum_i \sigma_i^z, \tag{1}$$

where $J > 0$ is the exchange coupling, $\boldsymbol{\sigma}_i = (\sigma_i^x, \sigma_i^y, \sigma_i^z)$, σ_i^μ are components ($\mu = x, y, z$) of the Pauli spin operators at ith site, $< i, j >$ denote sum over all pairs of nn spins and H is the longitudinal field.

Some years ago, a simple and versatile scheme, denoted by differential operator technique[21], was proposed and applied exhaustively to study a large variety of problems, in particular, to treat the criticality of quantum models[4, 9, 19] obtaining satisfactory results in comparison with more sophisticated methods (for example, Monte Carlo simulation). This method is used with a decoupling procedure which ignores all high-order spin correlations (*effective field theory*-EFT). The great advantages of this technique is the small CPU time and the possibility of obtaining good qualitative results using small systems. As a starting point, the averages of a general function involving spin operator components $\mathcal{O}(\{n\})$ are obtained by[4]

$$\langle \mathcal{O}(\{n\}) \rangle = \left\langle \frac{Tr_{\{n\}} \mathcal{O}(\{n\}) e^{-\beta \mathcal{H}_{\{n\}}}}{Tr_{\{n\}} e^{-\beta \mathcal{H}_{\{n\}}}} \right\rangle, \tag{2}$$

where the partial trace $Tr_{\{n\}}$ is taken over the set $\{n\}$ of spin variables (finite cluster) specified by the multisite spin Hamiltonian $\mathcal{H}_{\{n\}}$ and $\langle \cdots \rangle$ indicates the usual canonical thermal average.

The method treats the effects of the surrouding spins of a finite cluster with N spins through a convenient differential operator technique[21] such that, in contrast to the usual mean-field approximation (MFA) procedure, all relevant self-spin correlations are taken exactly into account. The interactions within the cluster are exactly treated and the effect of the remaining lattice spins is treated by a given approximation (here we use the random phase approximation-RPA). In order to treat the Hamiltonian (1), we use the four-site cluster approximation, given by

$$\mathcal{H}_4 = J \left(\boldsymbol{\sigma}_1 \cdot \boldsymbol{\sigma}_2 + \boldsymbol{\sigma}_2 \cdot \boldsymbol{\sigma}_3 + \boldsymbol{\sigma}_3 \cdot \boldsymbol{\sigma}_4 + \boldsymbol{\sigma}_4 \cdot \boldsymbol{\sigma}_1 \right) - \sum_{r=1}^{4} a_r \sigma_r^z, \tag{3}$$

where $a_r = -J \sum_{\boldsymbol{\delta}_r} \sigma_{r+\boldsymbol{\delta}_r}^z + H$ and $\boldsymbol{\delta}_r$ corresponds to nn vectors.

Substituting Eq. (3) in (2), we obtain the average magnetizations in sublattices A and B, respectively, by

$$m_A = \langle \sigma_1^z \rangle = \left\langle \frac{\partial \ln \mathcal{Z}_4(\mathbf{a})}{\partial(\beta a_1)} \right\rangle, \tag{4}$$

and

$$m_B = \langle \sigma_2^z \rangle = \left\langle \frac{\partial \ln \mathcal{Z}_4(\mathbf{a})}{\partial(\beta a_2)} \right\rangle, \tag{5}$$

with

$$\mathcal{Z}_4(\mathbf{a}) = Tr_{\{\boldsymbol{\sigma}\}} e^{-\beta \mathcal{H}_4}, \tag{6}$$

where $\mathbf{a} = (a_1, a_2, a_3, a_4)$ and $\{\boldsymbol{\sigma}\} = \{\boldsymbol{\sigma}_1, \boldsymbol{\sigma}_2, \boldsymbol{\sigma}_3, \boldsymbol{\sigma}_4\}$.

Using the identity $\exp(\mathbf{a} \cdot \mathbf{D}) f(\mathbf{x}) = f(\mathbf{x} + \mathbf{a})$, where $\mathbf{D} = (D_1, D_2, D_3, D_4)$ and $\mathbf{x} = (x_1, x_2, x_3, x_4)$ are four-dimensional differential operator and vector, respectively, $D_\mu = \frac{\partial}{\partial x_\mu}$, and also the van der Waerden identity for σ_i^z component Pauli spin operator, $\exp(\lambda \sigma_i^z) = \cosh(\lambda) + \sigma_i^z \sinh(\lambda)$, Eqs. (4) and (5) are rewritten as ($\mu = A$ or B)

$$\begin{aligned} m_\mu = \Bigg\langle & \prod_{\boldsymbol{\delta}_1}^{z-2} (\alpha_1 + \sigma_{1+\boldsymbol{\delta}_1} \beta_1) \cdot \prod_{\boldsymbol{\delta}_2}^{z-2} (\alpha_2 + \sigma_{2+\boldsymbol{\delta}_2} \beta_2) \cdot \\ & \prod_{\boldsymbol{\delta}_3}^{z-2} (\alpha_3 + \sigma_{3+\boldsymbol{\delta}_3} \beta_3) \cdot \prod_{\boldsymbol{\delta}_4}^{z-2} (\alpha_4 + \sigma_{4+\boldsymbol{\delta}_4} \beta_4) \Bigg\rangle f_\mu(\mathbf{x} + \mathbf{L})|_{\mathbf{x}=0} \end{aligned} \tag{7}$$

with

$$f_A(\mathbf{x}) = \frac{\partial \ln \mathcal{Z}_4(\mathbf{x})}{\partial x_1}, \tag{8}$$

$$f_B(\mathbf{x}) = \frac{\partial \ln \mathcal{Z}_4(\mathbf{x})}{\partial x_2}, \tag{9}$$

and

$$\mathcal{Z}_4(\mathbf{x}) = Tr_{\{\boldsymbol{\sigma}\}} e^{\mathcal{A}(\mathbf{x})}, \tag{10}$$

where $\mathbf{L} = \beta H(1,1,1,1)$, $\alpha_r = \cosh(K D_r)$, $\beta_r = \sinh(K D_r)$, $K = \beta J$ and the normalized operator $\mathcal{A}(\mathbf{x})$ is defined by

$$\mathcal{A}(\mathbf{x}) = -K \left(\boldsymbol{\sigma}_1 \cdot \boldsymbol{\sigma}_2 + \boldsymbol{\sigma}_2 \cdot \boldsymbol{\sigma}_3 + \boldsymbol{\sigma}_3 \cdot \boldsymbol{\sigma}_4 + \boldsymbol{\sigma}_4 \cdot \boldsymbol{\sigma}_1 \right) - \sum_{r=1}^{4} x_r \sigma_r^z. \tag{11}$$

The operator (11) can be written in matrix form, then using the basis of the $\{\sigma_r^z\}$ components for diagonalization, i.e., $\{|m_1, m_2, m_3, m_4\rangle, m_r = \pm 1\}$, we obtain the following

symmetrical block matrix

$$\mathcal{A}(\mathbf{x}) = \begin{bmatrix} \mathbf{A}^+ & 0 & 0 & 0 & 0 \\ 0 & \mathcal{B} & 0 & 0 & 0 \\ 0 & 0 & \mathcal{C} & 0 & 0 \\ 0 & 0 & 0 & \mathcal{B} & 0 \\ 0 & 0 & 0 & 0 & \mathbf{A}^- \end{bmatrix}_{16\times 16} , \tag{12}$$

with

$$\mathbf{A}^{\pm} = \mp(x_1 + x_2 + x_3 + x_4), \tag{13}$$

$$\mathcal{B} = \begin{bmatrix} b_{11} & -2K & 0 & -2K \\ -2K & b_{22} & -2K & 0 \\ 0 & -2K & b_{33} & -2K \\ -2K & 0 & -2K & b_{44} \end{bmatrix} \tag{14}$$

and

$$\mathcal{C} = \begin{bmatrix} c_{11} & -2K & 0 & 0 & -2K & 0 \\ -2K & c_{22} & -2K & -2K & 0 & -2K \\ 0 & -2K & c_{33} & 0 & -2K & 0 \\ 0 & -2K & 0 & c_{44} & -2K & 0 \\ -2K & 0 & -2K & -2K & c_{55} & -2K \\ 0 & -2K & 0 & 0 & -2K & c_{66} \end{bmatrix} , \tag{15}$$

where $b_{11} = -(x_1 + x_2 + x_3 - x_4)$, $b_{22} = -(x_1 + x_2 - x_3 + x_4)$, $b_{33} = -(x_1 - x_2 + x_3 + x_4)$, $b_{44} = -(-x_1 + x_2 + x_3 + x_4)$, $c_{11} = -(x_1 + x_2 - x_3 - x_4)$, $c_{22} = -(x_1 - x_2 + x_3 - x_4) + 4K$, $c_{33} = -(-x_1 + x_2 + x_3 - x_4)$, $c_{44} = -(x_1 - x_2 - x_3 + x_4)$, $c_{55} = -(-x_1 + x_2 - x_3 + x_4) + 4K$ and $c_{66} = -(-x_1 - x_2 + x_3 + x_4)$.

The matrix (12) is diagonalized numerically and then the functions $f_\mu(\mathbf{x})$ are obtained for a given value of the reduced temperature $t = 1/K$. On the other hand, Eqs. (7) are mathematically intractable because they involve an infinite number of coupled correlations functions. Here we use an approximation (RPA) which neglects correlations between different spins, i.e.,

$$\left\langle \sigma_i^z \cdot \sigma_j^z \cdot \cdots \cdot \sigma_l^z \right\rangle \simeq \left\langle \sigma_i^z \right\rangle \cdot \left\langle \sigma_j^z \right\rangle \cdot \cdots \cdot \left\langle \sigma_l^z \right\rangle , \tag{16}$$

where $i \neq j \neq ... \neq l$. Approximation (16) neglects correlations between different spins but takes relations such as $\left\langle (\sigma_i^z)^2 \right\rangle = 1$ exactly into account, while in the usual MFA all the self- and multi-spin correlations are neglected.

Using the approximation (16) in Eq. (7), we get the following set of state equations:

$$m_\mu = \Phi_\mu(m_A, m_B), \tag{17}$$

with

$$\begin{aligned}\Phi_\mu(m_A, m_B) \;=\; & (\alpha_1 + m_B\beta_1)^{z-2} \cdot (\alpha_2 + m_A\beta_2)^{z-2} \cdot \\ & (\alpha_3 + m_B\beta_3)^{z-2} \cdot (\alpha_4 + m_A\beta_4)^{z-2}\; f_\mu(\mathbf{x}+\mathbf{L})|_{\mathbf{x}=0}\,. \end{aligned} \tag{18}$$

The calculations of $\Phi_\mu(m_A, m_B)$ were performed analytically, where the coefficients of the expansion in terms of m_A and m_B powers are written as a function of $f_\mu(\mathbf{x})$, which is obtained numerically through of the diagonalization of the $\mathcal{A}(\mathbf{x})$ matrix, Eq. (12). The final expressions are too lengthy and will be omitted.

Defining the uniform $m = \frac{1}{2}(m_A + m_B)$ and staggered $m_s = \frac{1}{2}(m_A - m_B)$ magnetizations, we can show that, near the critical point $T_N(H)$ ($m_s \to 0$, $m \to m_o$), the magnetization in sublattice A is expanded up to linear order in m_s by

$$m_A \simeq A_0(T, H, m_o) + A_1(T, H, m_o)m_s + ... \tag{19}$$

where the coefficients $A_{r=0,1}(T, H, m_o)$ are given in Appendix A. Using the fact that $m_A = m_o + m_s$, from Eq. (19) we obtain

$$A_0(T, H, m_o) = m_o, \tag{20}$$

and

$$A_1(T, H, m_o) = 1. \tag{21}$$

III. RESULTS

The Néel temperature $T_N(H)$ is obtained if we simultaneously solve the set of two equations above, Eqs. (20) and (21), for each intensity of the external field H. For fixed coordination number (z), we determine the phase diagram in the $T - H$ plane that comprises a field-induced antiferromagnetic (AF) phase with $m_s \neq 0$ at low fields and paramagnetic (P) phase with $m_s = 0$ at high fields. In the limit of null field ($H = 0$), we have $m_A = -m_B$ ($m_o = 0$) and the Néel temperature is obtained by solving numerically only one equation

$A_1(T_N, 0, 0) = 1$. For the sc ($z = 6$) and bcc ($z = 8$) lattices we found by using EFT-4 (EFT-2) $k_B T_N(0)/J = 4.81$ (4.95) and 6.89 (6.94), respectively. Note that EFT-2 for a sc ($z = 6$) lattice was treated previously in Ref. 19, here we extend the method for the bcc ($z = 8$) lattice. Our results for $T_N(0)$on a bcc lattice can be compared with the $k_B T_N(0)/J = 5.53$ value obtained by using SE[17]. With increasing cluster size, we have observed a small convergence of the critical (Néel) temperature.

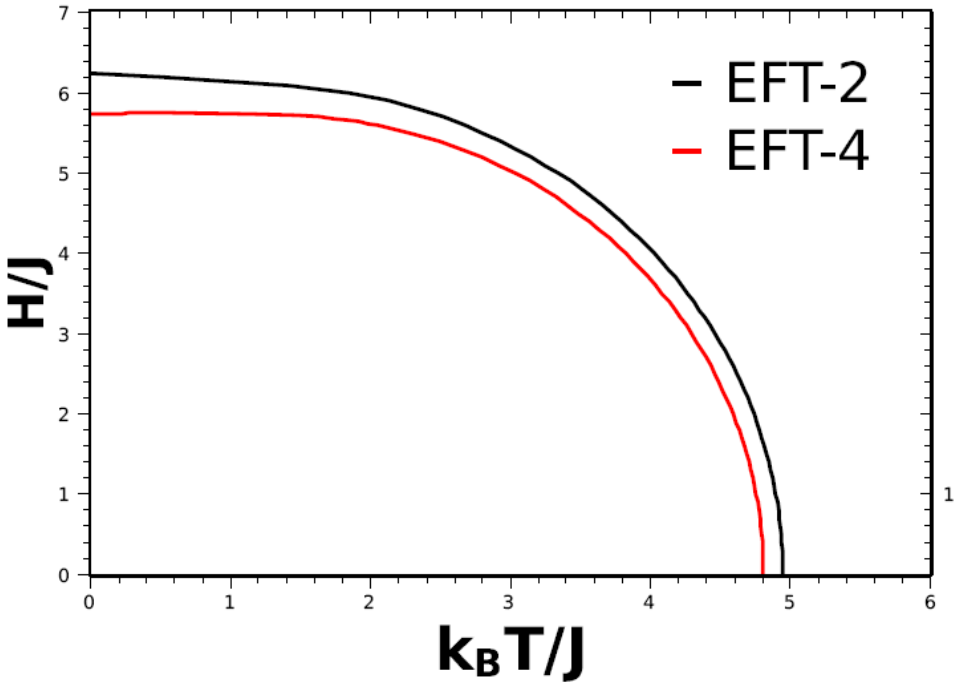

FIG. 1: Behavior of the reduced critical temperature $k_B T_N/J$ as a function of the reduced field H/J for the quantum spin-1/2 Heisenberg antiferromagnetic model on a simple cubic ($z = 6$) lattice. We present the results obtained bt the EFT-2 (Ref.19) and EFT-4 (present work) methods.

The results for the critical frontier of the quantum spin-1/2 Heisenberg antiferromagnet on a simple cubic ($z = 6$) lattice in the $T - H$ plane are shown in Fig. 1. We compare our results (EFT-4) with those obtained by using the EFT-2 method[19], where lines of second order phase transitions between the AF and P phases are observed. The critical behavior are different, where T_N approaching zero when the field increases to $H = H_c$ (critical field) with $H_c = 6.24J > 6J$ (**classical value**) and $H_c = 5.85 < 6J$ obtained by using EFT-2 and EFT-4, respectively. We found by larger cluster the expected result of the reduction of critical value due the quantum fluctuations at $T = 0$. The value for H_c by using EFT-2, in

principle wrong qualitatively, can be attributed to a finite size effect (cluster with $N = 2$ spins).

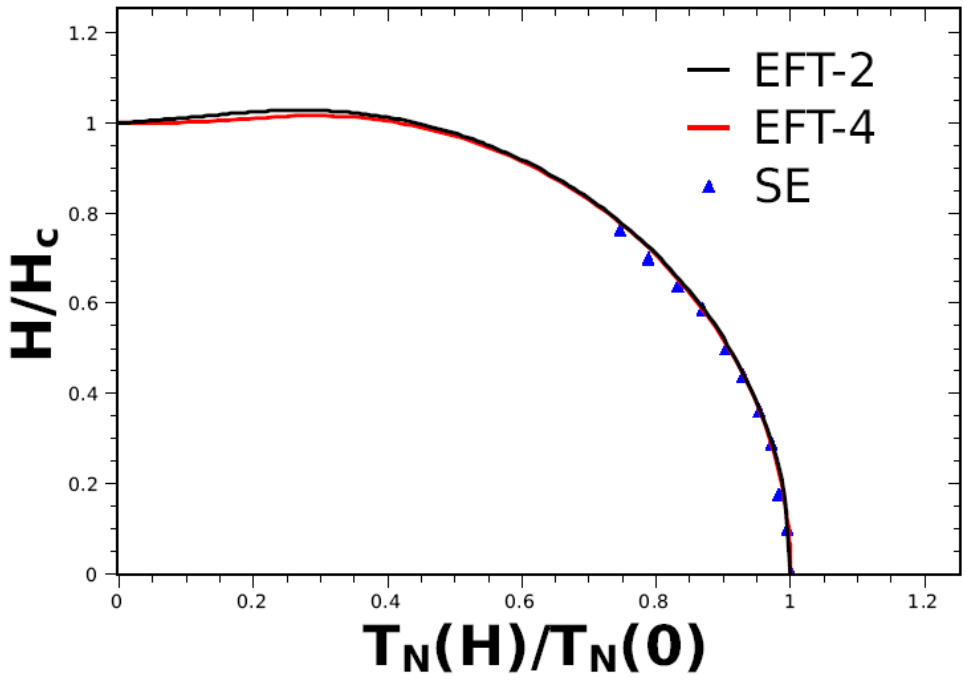

FIG. 2: Behavior of the reduced critical temperature $T_N(H)/T_N(0)$ as a function of the reduced field H/H_c of the quantum spin-1/2 Heisenberg antiferromagnetic model on a body-centered cubic ($z = 8$) lattice. We present the results from EFT-2 and EFT-4 methods both obtained in this works. We compare our results with series expansion (SE)[17].

To analyze the existence or not of reentrant behavior at low temperature in the phase diagram in the $T - H$ plane on a bcc lattice, in Fig. 2 we present the results obtained in this work by using EFT-2 and EFT-4. In the low field region, we compare our results with the SE[17] method. For a better comparison of results, we renormalize the field and temperature by the critical values at $T = 0$ (H_c) and $H = 0$ ($T_N(0)$), respectively. We observe a good qualitative accordance between our results (EFT-2 and EFT-4) and those obtained by using a rigorous method (SE). Quantum fluctuations decrease with increasing coordination number (z), finally disappearing in the limit $z \to \infty$ where MFA results are exact. The phase diagram for this model on a bcc lattice, obtained by using MFA[22], presents $H_c = 8J$. At low temperature, around the critical field H_c, we have observed a small reentrant behavior, with positive slope $a_c > 0$, and critical fields $H_c = 8.22J$ (EFT-2)

and $8.09J$ (EFT-4) in contrast with MFA results[22]. Using EFT-2 and EFT-4 we have found a reduced critical field $H_c/8J \simeq 1$, which is due to the small quantum effect when the value of z is increased, such that $\lim_{z\to\infty}(H_c/zJ) = 1$.

IV. CONCLUSION

We have studied the criticality of the quantum spin-1/2 Heisenberg antiferromagnetic model in the presence of a longitudinal field by using the differential operator technique in the effective field theory (EFT) in finite clusters ($N = 2, 4$). We obtained the phase diagram in the $T-H$ plane on sc and bcc lattices for all interval of field. At null temperature, we have found a critical field value H_c smaller than $6J$ (classical value) on a sc lattice by using EFT-4, while the EFT-2 method[19] obtain $H_c > 6J$. We expect a critical behavior $H_c < 6J$, and, therefore, the result obtained by using EFT-2, in principle wrong qualitatively, can be attributed due the finite size effect. On the other hand, we obtain on a bcc lattice, by using the two methods, a value of the critical field $H_c > 8J$. Since it is expected that H_c is smaller than $8J$, due to quantum fluctuations, we believe our result is a finite-size effect. As obtained for the sc lattice, we believe H_c will decrease if bigger cluster are used.

Appendix A

The coefficients $A_0(T, H, m_o)$ and $A_1(T, H, m_o)$ are defined by the expressions:

$$A_0(T, H, m_o) = \prod_{r=1}^{4} \left(\alpha_r + m_o\beta_r\right)^{z-2} f_A(\mathbf{x}+\mathbf{L})|_{\mathbf{x}=0}$$

and

$$A_1(T, H, m_o) = (z-1)\prod_{r=1}^{4} \left(\alpha_r + m_o\beta_r\right)^{z-2} \sum_{l\neq r}^{4} (-1)^l \beta_l \left(\alpha_l + m_o\beta_l\right)^{z-3} f_A(\mathbf{x}+\mathbf{L})|_{\mathbf{x}=0}$$

We have used in this work $z = 6$ and $z = 8$ to study the phase diagram in the $T - H$ plane for the sc and bcc lattices, respectively.

ACKNOWLEDGEMENT

This work was partially supported by CNPq, FAPEAM and CAPES (Brazilian Research Agencies). We are indebted to Dr. Nilton Branco of the Universidade Federal de Santa Catarina for their critical reading of this manuscript.

---

[1] E. Manousakis, *Rev. Mod. Phys.* **63**, 1 (1991).

[2] G. S. Rushbrooke and P. J. Wood, *Mol. Phys.* **6**, 409 (1963).

[3] R. Kubo, *Phys. Rev.* **87**, 568 (1952); T. Oguchi, *Phys. Rev.* **117**, 117 (1960); S. H. Liu, *Phys. Rev.* **142**, 266 (1966).

[4] J. Ricardo de Sousa and Ijanilio G. Araújo, *J. Magn. Magn. Mater.* **202**, 231 (1999); ibid *Solid State Commun.* **115**, 265 (2000); ibid *Phys. Lett. A* **272**, 333 (2000).

[5] G. Shirane, *et al. Phys. Rev. Lett.* **59**, 1613 (1987).

[6] Y. Endoh, *et al. Phys. Rev. B* **37**, 7443 (1988).

[7] G. Aeppli, et al. *Phys. Rev. Lett.* **62**, 2052 (1989).

[8] N. S. Branco and J. Ricardo de Sousa, *Phys. Rev. B* **62**, 5745 (2000).

[9] Ijanilio G. Araújo, J. Ricardo de Sousa, and N. S. Branco, *Physica A* **305**, 585 (2002).

[10] P. W. Anderson, *Phys. Rev.* **86**, 694 (1952).

[11] J. G. Bednorz and K. A. Muller, *Z. Phys. B* **64**, 189 (1986).

[12] P. W. Anderson, *Science* **235**, 1196 (1987).

[13] K. W. Mess, E. Lagendijk, D. A. Curtis, and W. J. Huiskamp, *Physica* (Amsterdam) **34**, 126 (1967).

[14] Zoltan Racz, *Phys. Rev. B* **21**, 4012 (1980).

[15] D. P. Landau, *Phys. Rev. B* **16**, 4164 (1977); ibid **14**, 255 (1976).

[16] Minos A. Neto and J. Ricardo de Sousa, *Phys. Rev. B* **70**, 224436 (2004).

[17] K. W. Pan, *Phys. Lett. A* **244**, 169 (1998).

[18] H. Falk, *Phys. Rev.* **133**, A1382 (1964).

[19] Edgar Bublitz Filho and J. Ricardo de Sousa, *Phys. Lett. A* **323**, 9 (2004).

[20] K. Okunishi, Y. Hieida, and Y. Akutsu, *Phys. Rev. B* **60**, R6953 (1999).

[21] R. Honmura and T. Kaneyoshi, *J. Phys. C* **12**, 3979 (1979).

[22] Edgar Bublitz and J. Ricardo de Sousa, *J. Magn. Magn. Mater.* **269**, 266 (2004).